Quaternary Science Reviews 58 (2012) 66–76

Contents lists available at SciVerse ScienceDirect

Quaternary Science Reviews

journal homepage: www.elsevier.com/locate/quascirev

Sahel megadrought during Heinrich Stadial 1: evidence for a three-phase evolution of the low- and mid-level West African wind system

Ilham Bouimetarhan [a,*], Matthias Prange [a], Enno Schefuß [a], Lydie Dupont [a], Jörg Lippold [b], Stefan Mulitza [a], Karin Zonneveld [a]

[a] MARUM – Center for Marine Environmental Sciences and Department of Geosciences, University of Bremen, PO Box 330 440, D-28334 Bremen, Germany
[b] Heidelberg Academy of Sciences, University of Heidelberg, D-69120 Heidelberg, Germany

ARTICLE INFO

Article history:
Received 15 December 2011
Received in revised form
28 September 2012
Accepted 12 October 2012
Available online

Keywords:
Heinrich Stadial 1
Sahel
Drought
Pollen
NE trade winds
African Easterly Jet
Mid-HS1 interlude

ABSTRACT

Millennial-scale dry events in the Northern Hemisphere monsoon regions during the last Glacial period are commonly attributed to southward shifts of the Intertropical Convergence Zone (ITCZ) associated with an intensification of the northeasterly (NE) trade wind system during intervals of reduced Atlantic meridional overturning circulation (AMOC). Through the use of high-resolution last deglaciation pollen records from the continental slope off Senegal, our data show that one of the longest and most extreme droughts in the western Sahel history, which occurred during the North Atlantic Heinrich Stadial 1 (HS1), displayed a succession of three major phases. These phases progressed from an interval of maximum pollen representation of Saharan elements between ~19 and 17.4 kyr BP indicating the onset of aridity and intensified NE trade winds, followed by a millennial interlude of reduced input of Saharan pollen and increased input of Sahelian pollen, to a final phase between ~16.2 and 15 kyr BP that was characterized by a second maximum of Saharan pollen abundances. This change in the pollen assemblage indicates a mid-HS1 interlude of NE trade wind relaxation, occurring between two distinct trade wind maxima, along with an intensified mid-tropospheric African Easterly Jet (AEJ) indicating a substantial change in West African atmospheric processes. The pollen data thus suggest that although the NE trades have weakened, the Sahel drought remained severe during this time interval. Therefore, a simple strengthening of trade winds and a southward shift of the West African monsoon trough alone cannot fully explain millennial-scale Sahel droughts during periods of AMOC weakening. Instead, we suggest that an intensification of the AEJ is needed to explain the persistence of the drought during HS1. Simulations with the Community Climate System Model indicate that an intensified AEJ during periods of reduced AMOC affected the North African climate by enhancing moisture divergence over the West African realm, thereby extending the Sahel drought for about 4000 years.

1. Introduction

Located at an important climatic transition zone between the hyper-arid Sahara desert in the north and the comparatively humid savanna in the south, the western Sahel is an ideal location to conduct late Quaternary paleoecological and paleoclimatic studies and to understand the interaction between low-latitude African monsoon regions and high-latitude climate change. On millennial timescales, the western Sahel region has experienced severe droughts in response to Northern Hemisphere high-latitude cooling during the last Glacial period (e.g. Street-Perrott and Perrott, 1990; Gasse, 2000; Jullien et al., 2007; Mulitza et al., 2008; Romero et al., 2008; Itambi et al., 2009). Recent reconstructions of the western Sahel climate indicate that a particularly arid interval of ~4000 years had occurred during HS1 in response to severe North Atlantic cold conditions (Mulitza et al., 2008; Niedermeyer et al., 2009) that, in turn, were induced by a slowdown of the AMOC (McManus et al., 2004). Such severe droughts have been associated with a southward shift of the ITCZ and its associated tropical rainbelt in conjunction with a strengthening of the NE trade winds that are also referred to as the "Harmattan" over North Africa (Dahl et al., 2005; Stouffer et al., 2006; Tjallingii et al., 2008; Itambi et al., 2009). Using a coupled climate model, Mulitza et al. (2008) explain the drying in West Africa with an additional mechanism involving intensification and southward expansion of the AEJ in combination with strengthened NE trades and

* Corresponding author. Tel.: +49 421 218 65138; fax: +49 421 218 65159.
E-mail address: bouimetarhan@uni-bremen.de (I. Bouimetarhan).

0277-3791/$ – see front matter © 2012 Elsevier Ltd. All rights reserved.
http://dx.doi.org/10.1016/j.quascirev.2012.10.015

a southward shift of the West African monsoon trough. However, the lack of proxy data with sufficient temporal resolution as well as the use of proxies unable to indicate source area changes did not allow the appropriate evaluation of the modeled hypothesis. Here we address this issue with a high-resolution palynological analysis from the continental slope off Northern Senegal to investigate shifts in vegetation and hydrological variability related to abrupt climate changes as well as changes in operating transport agents (wind and river). We conducted simulations with the Community Climate System Model to assess our palynological results in a physically consistent way. Both our pollen data and the numerical climate model experiment suggest a key role for the AEJ in stabilizing the western Sahel drought during HS1.

2. Regional setting and background

2.1. Continental climate

The climate of the Sahel is characterized by a strong hydrologic seasonality controlled mainly by the West African monsoon system with high rainfall during the boreal summer and arid conditions during winter (Nicholson, 2009) as a result of the latitudinal and seasonal migration of the ITCZ and its associated tropical rainbelt (Hsu and Wallace, 1976). Two main wind systems control the modern atmospheric circulation pattern over West Africa and thus are main transport agents of dust and terrestrial palynomorphs (Hooghiemstra and Agwu, 1986; Dupont, 1993). During boreal summer, when the ITCZ has migrated to its northernmost position, monsoonal flow is generated over NW Africa producing most of the rainfall (Nicholson and Grist, 2003). During that time, dust layers of Saharan particles are transported within the Saharan Air Layer from an easterly source westward toward the Atlantic Ocean by the AEJ. The mid-tropospheric AEJ reaches maximum wind speeds between 700 and 500 hPa in summer (Sarnthein and Koopmann, 1980; Prospero and Carlson, 1981; Prospero and Nees, 1986; Prospero, 1990; Prospero et al., 2002; Colarco et al., 2003; Stuut et al., 2005; Afiesimama, 2007) (Fig. 1). In comparison, the southern position of the ITCZ during the dry season in boreal winter results in the strengthening of the low-level NE trade winds blowing almost parallel to the coast (Sarnthein et al., 1981) delivering aeolian material from the dry northern areas (e.g., Mauritania, Sahara).

2.2. Modern vegetation patterns and pollen transport

Vegetation in West Africa gradually changes from desert to dense tropical rainforest reflecting the north-south mean annual precipitation gradient (Fig. 1). Five major floristic regions can be delineated (White, 1983): 1) Desert vegetation is mainly represented by pollen of Chenopodiaceae–Amaranthaceae (Cheno-Am) originating from the sparse vegetation in the Sahara and its fringes (Hooghiemstra and Agwu, 1986; Dupont and Agwu, 1991), 2) the semi-desert grassland and shrubland of Sahelian vegetation (dry savannah) made up by non-arboreal plants, particularly grasses that produce high amounts of pollen and thus dominate other pollen taxa from the savanna, and by woody species of the regional wooded grassland, such as *Boscia senegalensis* and *Acacia raddiana*, and herbs such as *Mitracarpus scaber* (Lézine, 1989), 3) the Sudanian savanna zone occurring in the southern part of the Sahel, 4) the tropical rainforest along the Gulf of Guinea, and 5) mangroves mainly in estuaries and near river mouths with distribution depending, inter alia, on salinity, river run-off and humidity (Hooghiemstra and Agwu, 1986; Dupont and Agwu, 1991; Lézine et al., 1995; Lézine, 1996).

In the NW African region, aeolian transport of pollen is mainly dependent on the low-level NE trade winds, but numerous studies

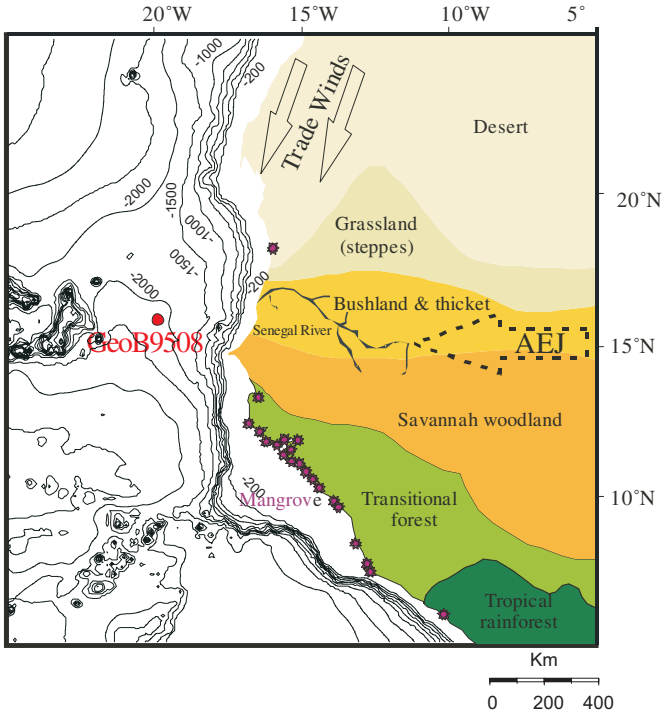

Fig. 1. Bathymetric map of the study area showing the location of marine core GeoB9508-5 and simplified phytogeography and modern vegetation distribution (after White, 1983). Arrows indicate predominant wind directions of northeasterly trade winds and the African Easterly Jet (AEJ, summer position) (after Sarnthein et al., 1982).

also document pollen and spore transport at the 600 hPa level by the mid-tropospheric AEJ (Hooghiemstra and Agwu, 1986; Hooghiemstra et al., 1987; Hooghiemstra, 1988; Dupont and Hooghiemstra, 1989; Dupont and Agwu, 1991; Dupont, 1999). The Senegal River, on the other hand, with its ~1790 km length and ~419,650 km^2 basin surface (World Resources Institute, 2003) is an important fluvial source of pollen and other terrestrial particles in the study area. Hooghiemstra et al. (2006) argue that the distribution of pollen over the ocean surface offshore NW Africa is reflected in the marine sediments without substantial displacement by marine currents.

3. Materials and methods

To trace the past wind system variability and assess source areas and dominant transport agents during HS1, we use the pollen content of core GeoB9508-5 (15°29.90′N, 17°56.88′W, ~2384 m water depth) retrieved from the continental slope off Northern Senegal westward of the Senegal River mouth (Mulitza et al., 2006) (Fig. 1). The total core length is ~956 cm composed of dark olive green mud. In this work, we present results for the section between ~314 and 134 cm covering the time interval ~20–12 cal kyr BP. The sediment colour in the studied interval is predominantly green with a short brown interval between 252 and 294 cm (Mulitza et al., 2006). The age model of the core, described in detail by Mulitza et al. (2008), is based on 12 AMS radiocarbon dates measured on samples of planktonic foraminifera and seven additional age control points derived by correlation of the benthic $\delta^{18}O$ record of our core GeoB9508-5 with that of core MD95-2042 (Shackleton et al., 2004). The HS1 was delimited in the studied core between ~19 and 15 kyr BP based on variations in the composition of the terrigenous material measured by XRF scanning (Mulitza et al., 2008) especially the iron-potassium (Fe/K) ratios suggested to vary with changes in humidity and monsoonal precipitation. The Fe/K ratios exhibit

millennial-scale variations coinciding with Heinrich stadials. Times of strong-AMOC weakening (HS6-HS1) are generally characterized by low Fe/K ratios, indicative of dry conditions over West Africa (Mulitza et al., 2008). The HS1 is also determined during the same time interval based on variations of *Cibicidoides wuellerstorfi* (also named *Planulina wuellerstorfi*) and alkenone sea surface temperature estimates (Niedermeyer et al., 2009).

3.1. Terrestrial proxy analysis

Pollen samples were taken every 5 cm for the time interval ~20–12 kyr BP resulting in an average temporal resolution of ~200 years. Samples (2 cm^3) were prepared for palynological processing using standard laboratory procedures (Faegri and Iversen, 1989) including decalcification with 10% hydrochloric acid (HCl) and removal of the siliceous fraction with 40% hydrofluoric acid (HF). One tablet of exotic *Lycopodium* spores (18,583 ± 1708 spores/tablet) was added to the samples during the decalcification process in order to calculate palynomorph concentrations and accumulation rates (see details in Bouimetarhan et al., 2009). After chemical treatments, samples were sieved through a 5 μm nylon mesh screen using an ultrasonic bath (maximum ~ 60 s) to disintegrate lumps of organic matter. A 40–60 μl aliquot was mounted on a permanent slide using glycerine jelly. One to four slides per sample were counted under a light microscope at 400× and 1000× magnification. Pollen grains were identified following Bonnefille and Riollet (1980) and Vincens et al. (2007) and the reference collection of the Department of Palynology and Climate Dynamics of the University of Göttingen. Pollen taxa are listed in Table 1 and total counts per sample (including herbs, shrubs, trees, and aquatics) are specified in the Supplementary Table. Other microfossils such as fresh water algae (*Botryococcus*, *Cosmarium*, *Pediastrum*, *Scenedesmus* and *Staurastrum*) were also counted but not included in the sum on which the pollen percentage calculations are based.

3.2. Design of the numerical climate model experiment

A numerical freshwater-hosing experiment with a readjusted version of the "paleo release" of the NCAR (National Center for Atmospheric Research) Community Climate System Model CCSM2.0.1 referred to as CCSM2/T31x3a (Prange, 2008) was performed as described by Mulitza et al. (2008). The global climate model is composed of four components representing atmosphere, ocean, land, and sea ice. The resolution of the atmospheric component is given by T31 (3.75° transform grid) spectral truncation for 26 layers, while the ocean has a mean resolution of 3.6° by 1.6° with 25 levels. The latitudinal resolution of the oceanic model grid is variable, with finer meridional resolution near the equator (0.9°). In this experiment, the present-day control run of CCSM2/T31x3a (Prange, 2008) was perturbed by a freshwater flux of 0.1 Sverdrup ($1\ Sv = 10^6\ m^3\ s^{-1}$) into high northern seas (i.e. Labrador Sea, Nordic Seas, Arctic Ocean, Hudson Bay, and Baffin Bay). The freshwater forcing caused a substantial weakening of the AMOC which, in turn, induced a southward shift of the West African monsoon trough associated with a strengthening of the low-level NE trades over North Africa, an intensification of the mid-tropospheric AEJ and, hence, a dramatic reduction of rainfall in the Sahel region (Mulitza et al., 2008). The continuously perturbed model was integrated for ~450 years so that the climate system could largely adjust to the freshwater forcing anomaly. In this study, we are interested in the temporal evolution of the trade winds and the AEJ during a climatic transition from a weak-AMOC state to a stronger-AMOC state. We therefore extended the numerical experiment by an additional 400-year integration phase in which the anomalous freshwater forcing was removed such that the AMOC could slowly recover. Given the use of present-day rather than deglacial boundary conditions and the highly idealized character of the freshwater perturbation, our model experiment should be considered as a sensitivity study. The goal of this numerical experiment is not to simulate the HS1 monsoonal system over Africa as accurate as possible, but rather to study the response of the West African wind system to changes in AMOC strength and, in particular, to examine the relationship between mid-level AEJ and low-level trade wind variations.

Table 1
List of identified pollen taxa in marine core GeoB 9508-5. Taxa are grouped according to their phytogeographical assignment.

Vegetation (Family)	Genus/species	Life form
Poaceae	Genus indet. (25 μm) Genus indet.	Herb
Cyperaceae	Various species	Herb
Mangrove		
Rhizophoraceae	*Rhizophora*	Tree
Rivers and swamps		
Typhaceae	*Typha*	Herb
Desert		
Amaranthaceae/ Chenopodiaceae (Cheno-Am)	Various species	Herb
Semi-desert		
Asteraceae	Various Asteroideae species	Herb
Asteraceae	*Artemisia*	Herb, shrub
Ephedraceae	*Ephedra distachya* -type	Shrub
Grasslands, woodlands, wooded grasslands of Sahel zone		
Rhamnaceae	*Ziziphus*-type	Shrub, tree
Capparaceae	*Boscia*-type	Shrub
Mimosaceae	*Mimosa*-type	Shrub
	Acacia	Shrub, tree
Rubiaceae	*Mitracarpus*	Herb
Sudanian and Guinean savanna		
Rubiaceae	*Borreria (=Spermacoce)*	Shrub
Asteraceae	*Vernonia*-type	Shrub
Ulmaceae	*Celtis*	Tree
Guinean forest		
Phyllanthaceae	*Uapaca*	Tree
Rubiaceae	*Psydrax* type *subcordata*	Tree
Rubiaceae	*Galium*	Herb
Other elements		
Euphorbiaceae	Various species	Tree, herb, shrub
Oleaceae	*Olea*	Tree
Pinaceae	*Pinus*	Tree

4. Results and interpretations

4.1. Palynological reconstructions

4.1.1. Description of the pollen assemblages

The pollen record from sediment core GeoB9508-5 over the last deglaciation (~20–12 kyr BP) shows large and abrupt changes in pollen concentrations and relative abundances as well as the dominance of the main taxa (Fig. 2). A total of 22 pollen taxa were identified (Table 1) with an average pollen count of 200 grains per sample ranging from 52 to 688. The quantitative pollen analysis shows an average concentration of ~19 × 10^2 grains/cm^3 and an average accumulation rate of ~65 grains/cm^2/yr. Varying between ~4 × 10^2 and ~60 × 10^2 grains/cm^3 on the studied sedimentary record, pollen concentrations reach maximum values at the latter part of HS1 (Fig. 2).

From the beginning to the end of the sequence, assemblages are dominated by Cyperaceae pollen reaching up to ~55% at the end of

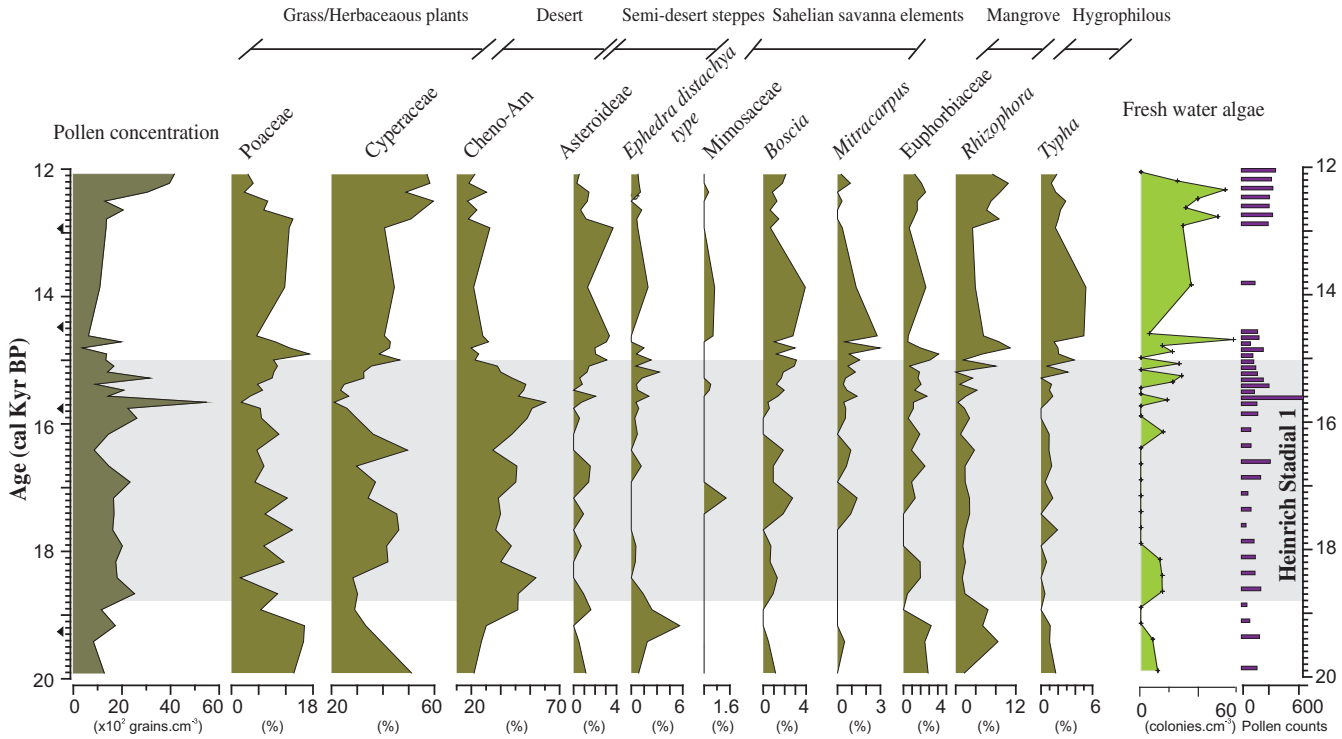

Fig. 2. Palynological data from marine sediment core GeoB9508-5 showing pollen concentrations ($\times 10^2$ grains cm^{-3}), relative abundances of selected taxa (%) and freshwater algae concentrations (colonies.cm^{-3}). Pollen abundances are calculated as percentages of the sum of total pollen including trees, shrubs and aquatic pollen. Heinrich Stadial 1 is indicated by the grey horizontal shading. Note the scale changes in *x*-axes. Triangles indicate age control points.

the sequence and Poaceae (grasses) pollen reaching a maximum of 18% at the bottom parts (Fig. 3). Cheno-Am pollen dominate the middle part of the diagram which coincides with HS1 accounting for up to 70% of the total pollen sum and reaching the highest accumulation rates with ~160 grains/cm^2/yr (Fig. 4). This interval also shows low values of fresh water algae concentrations and accumulation rates. Additionally, *Rhizophora* pollen percentages decrease from ~8 to 1.3% while *Typha* pollen shows an average abundance of ~1% (Fig. 2).

Cheno-Am pollen percentages rapidly increase from ~20 up to 62% at the onset of HS1 and reach their first maximum in the pollen record at ~18.4 kyr BP when grass pollen decline to 1% (Figs. 2 and 3). Cheno-Am pollen percentages subsequently decrease to 30% (17.4 kyr BP), allowing Cyperaceae pollen to become dominant (~50%), but then increase again up to 70% toward the end of HS1 (maximum at ~15.6 kyr BP). Sahelian savanna elements such as *Boscia* and *Mitracarpus* have higher relative pollen abundances between ~17.4 and 16.2 kyr BP together with a slight increase in their accumulation rates (Fig. 4c). After the HS1 at ~15 kyr BP, Cyperaceae pollen dominate the pollen assemblage while Cheno-Am pollen percentages show their lowest values (~17–30%). Hygrophilous taxa such as *Typha* pollen increase to 6% accompanied with higher input of Sahelian elements (e.g., *Boscia*, Mimosaceae and *Mitracarpus* pollen) which comprise ~9% of the total pollen sum along with other pollen taxa such as Euphorbiaceae, Mimosaceae, Asteroideae. Similarly, *Rhizophora* pollen percentages increase to ~12% (Fig. 2).

4.1.2. Interpretation of the pollen record

In the studied sequence, Cheno-Am pollen percentages started to increase under the extremely arid conditions of HS1 (Fig. 3e). This interval of dominating Saharan pollen percentages corresponds to a period generally characterized by lower $\delta^{13}C$ values of tests of *C. wuellerstorfi* recorded in the same sediment core by Niedermeyer et al. (2009) (Fig. 3b) indicating reduced deepwater ventilation due to AMOC weakening (Duplessy and Shackleton, 1985; Duplessy et al., 1988). Coincident with this timing, $^{231}Pa/^{230}Th$ ratios recorded in Bermuda Rise sediment core GGC5 (McManus et al., 2004) (Fig. 4g) as well as in other sediment cores of the Atlantic Ocean (Gherardi et al., 2005, 2009; Lippold et al., 2012) suggest substantial AMOC weakening providing a connection regarding the strength of the AMOC to the severe aridity of HS1.

Chenopodiaceae and Amaranthaceae are today the plant families that host the most common representatives of desert vegetation in the Sahara and its fringes (Hooghiemstra and Agwu, 1986) and produce large amounts of pollen grains, which overwhelm the production of other taxa present in the Sahara. The main season of pollen release in the northern fringe of the Sahara is during the winter when the NE trade winds are strong (Hooghiemstra and Agwu, 1986; Hooghiemstra, 1988). Thus, the conditions for Cheno-Am pollen transport to the continental slope off Senegal by the NE trade winds are optimal (Dupont and Agwu, 1991). Therefore, the expansion of Saharan vegetation during the extremely dry HS1 is associated with NE trade wind intensification over the western Sahel during intervals of reduced AMOC. This pattern is consistent with the sharply reduced monsoonal precipitation as indicated by low Fe/K values within sediment core GeoB9508-5 that correspond to decreased fluvial input and enhanced dust supply (Mulitza et al., 2008) (Fig. 4f). A similar trend has also been inferred further north at the Mauritanian margin and off Morocco where the maximum dust supply occurred during HS1 (Jullien et al., 2007; Penaud et al., 2010).

The important feature within HS1 in the western Sahel is that the Cheno-Am pollen values rise sharply (>40%) and abruptly (within ~200 years) to peak values in the first phase from ~19 to

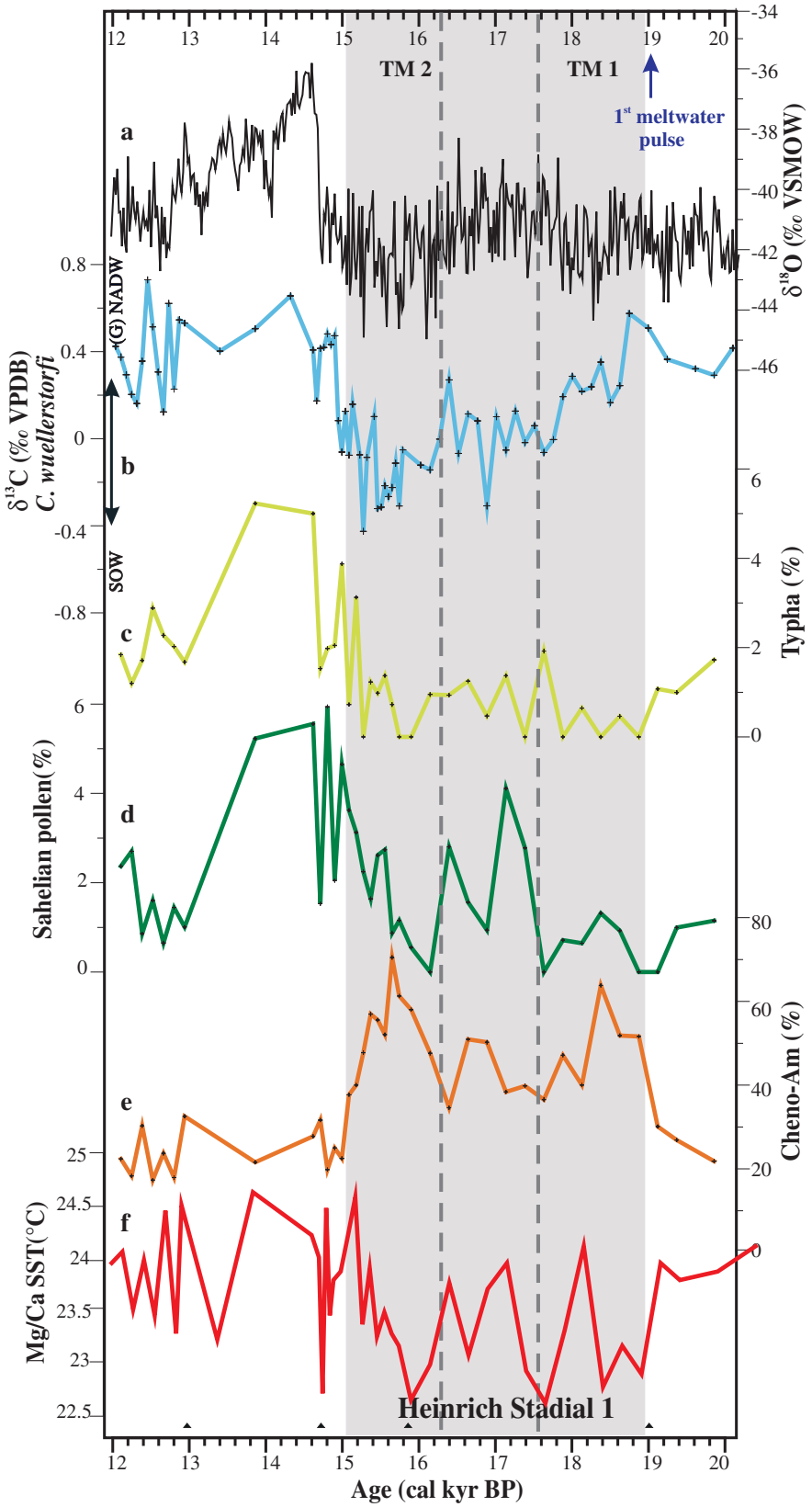

Fig. 3. Deglaciation records of (a): $\delta^{18}O$ of the North Greenland Ice Core Project (NGRIP members, 2004), (b): $\delta^{13}C$ of *Cibicidoides wuellerstorfi* from core GeoB9508-5 (Niedermeyer et al., 2009) indicating relative changes in (glacial) North Atlantic Deep Water ((G)NADW) and deep Southern Ocean Water (SOW), (c): relative abundances of *Typha* pollen, (d): relative abundances of Sahelian pollen represented by *Boscia* and *Mitracarpus*, (e): relative abundances of desert pollen represented by Chenopodiaceae–Amaranthaceae (Cheno-Am), (f): Mg/Ca-based sea surface temperature from core GeoB9508-5 (Zarriess et al., 2011). Shading indicates the interval of HS1 and the dashed lines denote its three phases. TM1 and TM2 stand for North East trade wind maximum 1 and 2, respectively. Triangles indicate age control points.

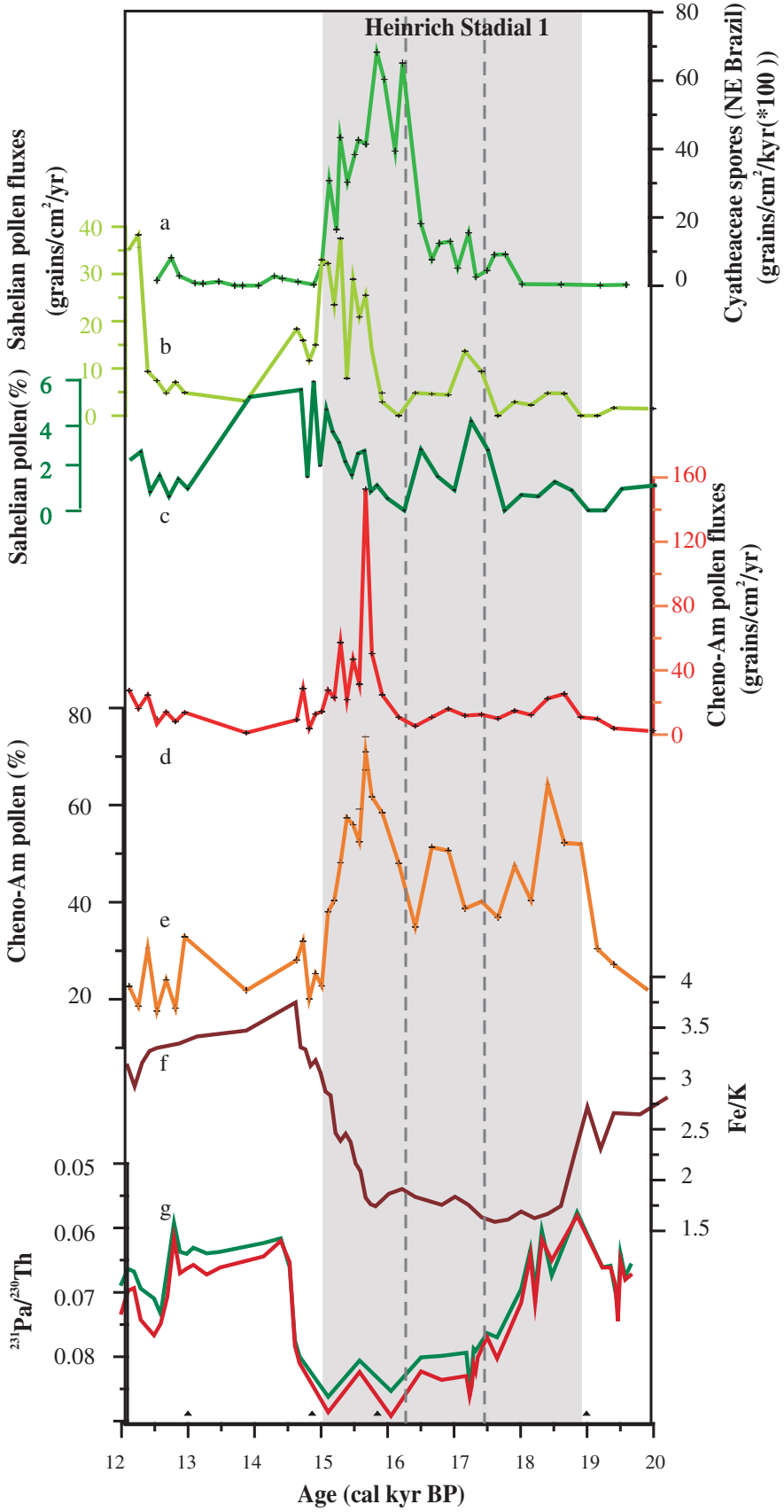

Fig. 4. Deglaciation record of (a): accumulation rates of non-degraded Cyatheaceae spores from core GeoB3910-2 representing more run-off and increase of humid forest in NE Brazil during the latter part of HS1 (Dupont et al., 2010), (b) accumulation rates of Sahelian pollen, (c): relative abundances of Sahelian pollen, (d): accumulation rates of Cheno-Am (Saharan) pollen, (e): Cheno-Am pollen percentages, (f): bulk Fe/K ratio from core GeoB9508-5 (Mulitza et al., 2008) indicating dry conditions in the Sahel during HS1, (g): sedimentary $^{231}Pa/^{230}Th$ from core GGC5 indicating reduced AMOC during HS1 (McManus et al., 2004). Shading indicates the interval of HS1 and the dashed lines denote its three phases. Triangles indicate age control points.

17.4 kyr BP (peak at ~18.4 kyr BP) and to even greater values in the later part from ~16.2 to 15 kyr BP (peak at ~15.6 kyr BP), which sandwich an interval of reduced input of Saharan pollen between ~17.4 and 16.2 kyr (Fig. 3e) showing that HS1 is a complex period consisting of three distinct phases.

Our results corroborate the findings of previous published records showing that HS1 displays an internal complexity consisting of a multi-step structure reported from the European margin, NE Brazil and the western USA (Bard et al., 2000; Grousset et al., 2001; Zaragosi et al., 2001; Peck et al., 2006; Eynaud et al., 2007; Naughton et al., 2007; Broecker et al., 2009; Naughton et al., 2009; Dupont et al., 2010; Stanford et al., 2011). However, the most striking feature of the HS1 in our record is the millennial interlude (~17.4–16.2 kyr BP) that is characterized by somewhat lower Saharan pollen content. This interval is aligned with a period of increased abundance of *Mitracarpus* pollen originating from the boundary between the Sahelian and Sudanian vegetation zones (Lézine and Hooghiemstra, 1990; Hooghiemstra et al., 2006) and *Boscia* pollen (Fig. 3d), which is common for the present-day Sahel vegetation and the northern part of the savannah woodland and wooded grasslands (Dupont and Agwu, 1991; Vincens et al., 2007) (Fig. 1). Both pollen types are mainly transported by the mid-level AEJ wind system (Dupont and Agwu, 1991).

On the basis of only relative abundances, one could argue that pollen taxa variations during HS1 could be simply due to the decrease/increase in inputs of other pollen rather than a signal of a changed climate regime. However, the relative abundances compare well with the pollen accumulation rates. Fig. 4d and e shows that Cheno-Am accumulation rates display similar trends with a small but clear increase at the onset of HS1 and maximum values at the end of HS1, constraining a mid-HS1 interlude of reduced input (see also the Supplementary Material). This interlude is marked by high values of both relative abundance and accumulation rates of Sahelian elements. Without considering any additional information, one might interpret the higher Sahelian pollen abundances as the result of a change in vegetation cover due to less severe aridity. Because, however, no significant increase in both pollen from hygrophilous vegetation (*Typha*, Fig. 3c) nor fresh water algae (Fig. 2) requiring wetter conditions and perennial freshwater is observed during the interlude, the change in pollen assemblage does not indicate an enhanced freshwater input by increased precipitation during the mid-HS1. The Fe/K record of GeoB9508-5 (Fig. 4f; Mulitza et al., 2008) as well as geomorphological studies by Michel (1973) provide another line of evidence that no reactivation of the Senegal River occurred and that humidity in the western Sahel remained very low, including the interlude between ~17.4 and 16.2 kyr BP. During the period between ~19 and 15 kyr BP, the development of the Ogolian dunes covering much of Senegal indicates a much drier climate in the western Sahel (Michel, 1973). Therefore, instead of an indication of more humid conditions, the Sahelian pollen maxima rather suggest a change in source area to more southern latitudes during the mid-HS1 interlude, thereby capturing pollen from a less arid region. Such a change would involve a shift in the predominant wind direction from northeasterly to easterly and imply a dominance of the AEJ over the NE trade winds.

After HS1, the observed increase of *Rhizophora* pollen percentages might reflect either the expansion of mangrove vegetation along the Senegal River delta or erosion of mangrove peat during sea-level rise. The latter interpretation, however, is less likely because the maximum pollen representation of *Rhizophora* occurs almost a millennium prior to the global sea-level rise associated with meltwater pulse 1A at ~14 ka BP (Fairbanks, 1989; Bard et al., 1990). The expansion of mangroves could be explained by reduced freshwater flow and a subsequent increase in marine influence that would have allowed mangroves to considerably extend within estuaries (Lézine and Casanova, 1989) and would also imply dry climatic conditions. An alternative explanation would be associated with the efficient transport by the Senegal River (Dupont and Agwu, 1991; Lézine et al., 1995; Lézine, 1996) and would instead require locally wetter conditions and a continuous input of freshwater, which would also fit the high values of *Typha* pollen and high accumulation rate values of fresh water algae during this time interval (Fig. 2). Thus, we suggest a return to more humid conditions with high fluvial activity and more moist continental conditions coinciding with the onset of the Bølling–Allerød warm period at high northern latitudes.

4.2. Results of the numerical experiment

The results of our freshwater-hosing experiment reveal that the strong reduction of the AMOC (due to freshwater input into the high-latitude northern seas) is associated with enhanced NE trades and a strong and southward expanded AEJ over the tropical North Atlantic/West African realm (Fig. 5a and b). After removal of the freshwater perturbation, the AMOC fully recovers after ~400 years. Likewise, Sahel precipitation, trade wind strength over West Africa, and the speed of the AEJ approach the values of the unperturbed control run (i.e. the strong-AMOC state) (Fig. 6). The key result of the numerical experiment is, however, that the two wind systems develop independently from each other rather than synchronously (Fig. 6c and d).

After removal of the freshwater perturbation and when the AMOC partly recovers, the trade winds relax very quickly and are adjusted after ~150 years (Figs. 5c and 6c) while rainfall in the Sahel is still strongly reduced (Figs. 6b and 7). Although Fig. 6c shows annual-mean trade wind strength, we note that this temporal behavior is also simulated for the winter season when the trades are strongest and the ITCZ is at its southernmost position (not shown). By contrast, only minor trends can be observed in the AEJ during this phase. As a result, an interval associated with an intermediate AMOC strength, which serves as our analogue for the mid-HS1 interlude observed in the pollen data, emerges during which the NE trades are almost as weak as in the strong-AMOC state, while the mid-troposphere still experiences a strong AEJ (Fig. 5d) (grey box in Fig. 6). A strong AEJ diverges moisture from continental Africa toward the Atlantic Ocean (e.g. Rowell et al., 1992; Cook, 1999; Rowell, 2003; Cook and Vizy, 2006; Patricola and Cook, 2007, 2008; Mulitza et al., 2008), thus maintaining dry conditions over West Africa during the intermediate-strength AMOC state (Fig. 7). It is only when the AEJ relaxes that drought conditions in West Africa abate.

Modern observational data show that changes in AEJ strength between extremely wet (1958–61) and dry (1982–1985) phases are about 2 m/s (e.g. Grist and Nicholson, 2001). Rowell (2003) has further shown that the AEJ is about 0.5–2 m/s weaker-than-normal during extremely wet Sahel years. Changes in our model experiment are of the same order of magnitude. However, the anomaly of HS1 lasted for several millennia rather than for only a few years, thus leaving a strong imprint on the pollen record.

5. Discussion

5.1. The HS1 as a "complex" episode including three major phases

The results of our numerical modeling experiment and palynological reconstructions corroborate the extremely dry conditions in western Sahel during HS1 suggested by previous studies from the Sahel/Sahara region (Lézine et al., 1995; Gasse, 2000; Mulitza et al., 2008; Romero et al., 2008; Itambi et al., 2009; Niedermeyer

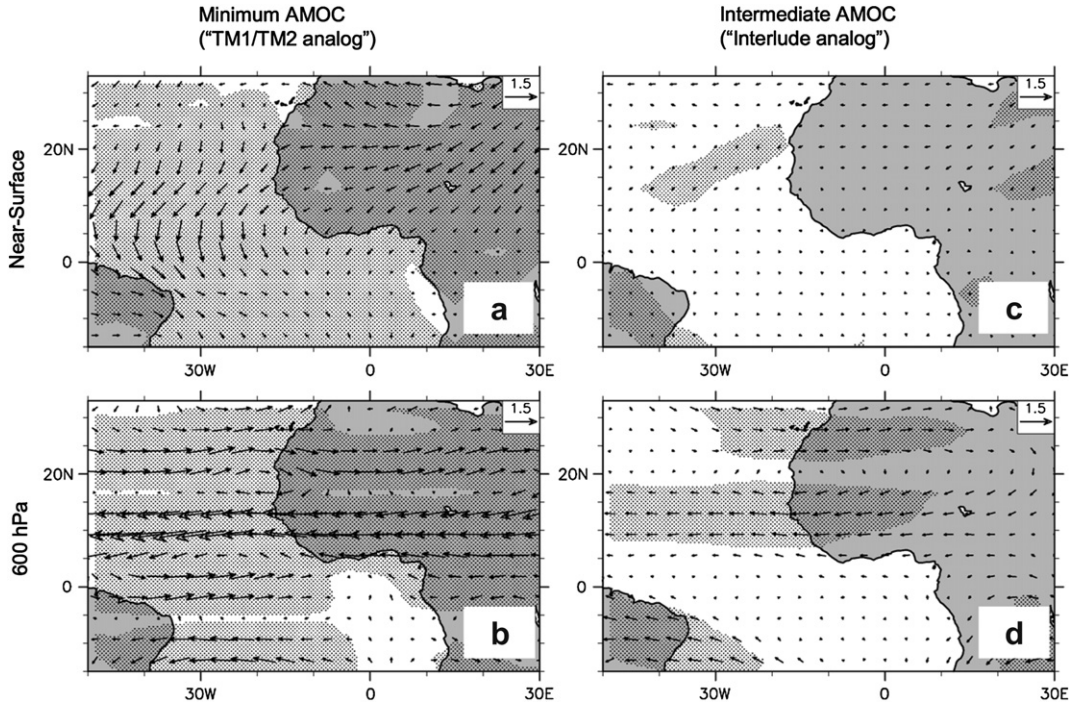

Fig. 5. Simulated wind anomalies (m/s) from a water-hosing sensitivity experiment with the Community Climate System Model, version CCSM2/T31x3a. (a, b): Wind anomalies associated with a strong (i.e. by 65%) reduction of the AMOC, (c, d): wind anomalies associated with an intermediate (i.e. by 30%) reduction of the AMOC. Near-surface wind anomalies represent annual means (a, c). Since the mid-tropospheric AEJ over West Africa is only a summer feature (Afiesimama, 2007), the plotted wind anomalies at 600 hPa represent the July–September season (b, d). All wind anomalies are based on 50-year averages taken from the transient climate model experiment as depicted in Fig. 6. Stippling indicates statistical significance of the meridional (a, c) and zonal (b, d) wind components at the 0.05 level based on a *t*-test (Fisher, 1925).

et al., 2009). Moreover, our results indicate that this 4000-year-long period (Mulitza et al., 2008) was not as uniform as previously thought and clearly shows a succession of three major phases.

The first phase of HS1 is dominated by Cheno-Am (Saharan) pollen and is correlated with an interval of strong NE trade winds and a southward expanded AEJ during initial AMOC weakening due to meltwater pulses in the North Atlantic that started around ~19 kyr BP (Clark et al., 1996). As a result, monsoonal rainfall retreated from the western Sahel leading to arid conditions and desert expansion. In contrast, a mid-HS1 millennial interlude (between ~17.4 and 16.2 kyr BP) showed minimum representation of Cheno-Am in the pollen record and increased input of Sahelian pollen is identified. This is interpreted as an interval of relaxed NE trade winds but still intense AEJ.

According to the model experiment, these variations can be explained by reduced cooling in the North Atlantic owing to a partial recovery of the AMOC. Indeed, the surface temperature record of GeoB9508-5 based on Mg/Ca of *Globigerinoides ruber* (pink) (315–400 μm) (Zarriess et al., 2011) supports the notion of milder North Atlantic temperatures during the mid-HS1 interlude (Fig. 3f), as does the $\delta^{18}O$ record from the North Greenland ice core (Fig. 3a, NGRIP members, 2004). However, to our knowledge, no paleoceanographic evidence has yet clearly documented such a partial recovery state of the AMOC during that period (Fig. 4g; McManus et al., 2004), even though the $\delta^{13}C$ record of tests of *C. wuellerstorfi* from GeoB9508-5 (Fig. 3b; Niedermeyer et al., 2009) shows a small rise during the mid-HS1 interlude, which might be interpreted to represent a partial recovery of glacial North Atlantic Deep Water (NADW) formation (Niedermeyer et al., 2009). While in our idealized model experiment North Atlantic temperature changes are simply controlled by AMOC variations, additional processes may also have influenced North Atlantic surface temperatures in reality. The mid-HS1 interlude identified in our pollen record coincides approximately with the phase of maximum input of ice-rafted debris (IRD) from the Laurentide ice-sheet into the mid-latitude North Atlantic (e.g. Jullien et al., 2006), i.e. the Heinrich event *sensu stricto* (Stanford et al., 2011). We hypothesize that the massive melting of icebergs created a shallow freshwater lens over the North Atlantic IRD belt. The increased stratification would have amplified the seasonal surface temperature contrast (cf. Haug et al., 2005) resulting in enhanced North Atlantic summer surface temperatures that may provide an alternative explanation for the mid-HS1 interlude during the West African monsoon season. On the other hand, surface temperature variations at site GeoB9508-5 (Fig. 3f) may be interpreted as a response to trade wind-induced changes in upwelling. Coastal upwelling might have influenced the core site during HS1, when the sea-level was lower than today (about 110–120 m (Lambeck and Chappell, 2001)) and, hence, the core location closer to the shoreline. The coldest temperatures during phases of trade wind maxima (Fig. 3f) would then be associated with enhanced upwelling of cold water, while the milder phase during the mid-HS1 interlude would be consistent with trade wind relaxation and less upwelling.

5.2. Intensified atmospheric circulation during HS 1

Both the data and model simulation suggest that the atmospheric and oceanographic systems were strongly coupled during the HS1 as a whole and particularly during the mid-HS1 interlude phase. It should be noted that the Sahel drought during this interval is still severe (the intermediate AMOC-strength interval exhibits only ~50% recovery of rainfall in the model experiment; see also Fig. 7), although the NE trades which transport dry Saharan air to the Sahel region, being a potentially important factor in driving the Sahel drought, have already weakened. The strong AEJ, however, still exported large amounts of moisture from the African continent

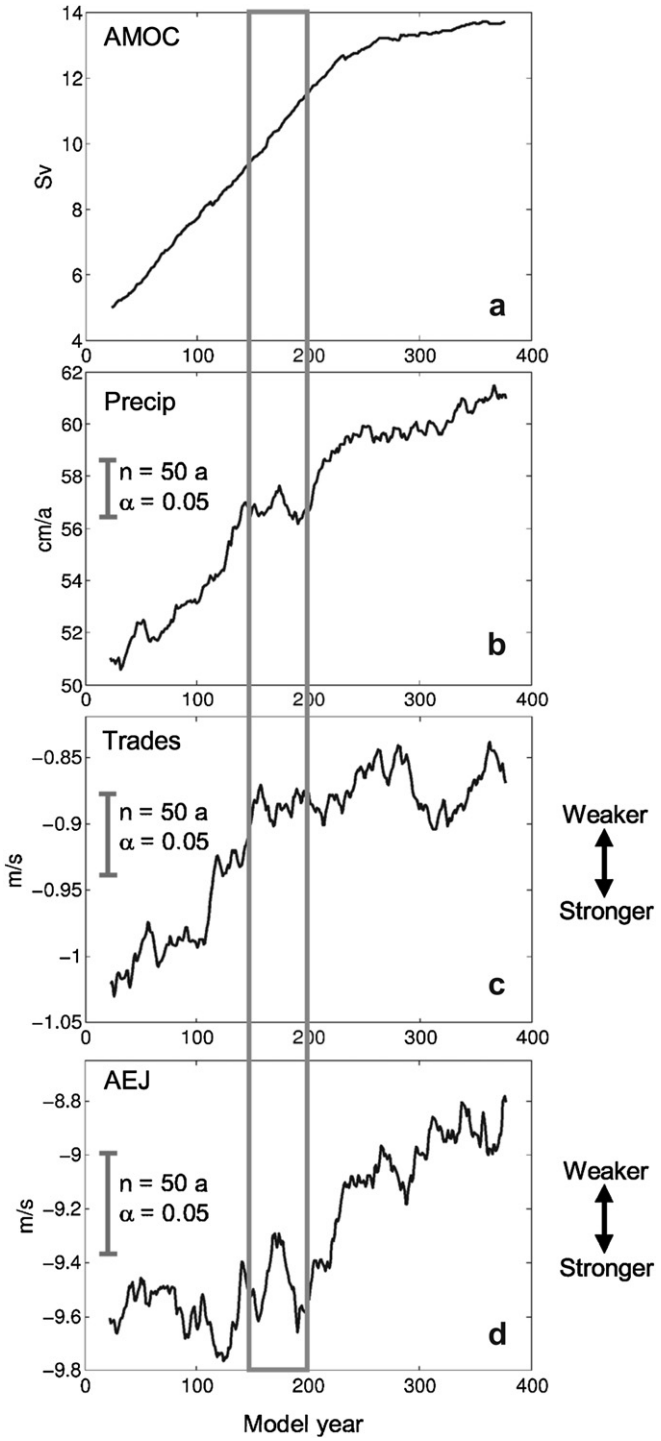

Fig. 6. Temporal evolution of relevant metrics after removal of the freshwater perturbation in a water-hosing experiment with CCSM2/T31x3a. (a): Maximum of the Atlantic meridional overturning streamfunction at 30°N below 800 m water depth. (b): Annual-mean precipitation averaged over the western Sahel (15°W–10°E, 10–20°N). (c): Annual-mean meridional near-surface wind velocity at 15°N averaged over 15°W–10°E as an index for the low-level trade wind strength in West Africa. (d): Summer-mean (July–September) zonal 600-hPa wind velocity averaged over the western Sahel (15°W–10°E, 10–20°N) as an index for the strength of the mid-tropospheric AEJ. All timeseries are smoothed by a 50-year boxcar average and start from the weak-AMOC state produced by the water-hosing. The grey box marks the 50-year interval over which the anomalous (against the strong-AMOC control run) fields shown in Fig. 5c and d are averaged and which is characterized by an AMOC of intermediate-strength. The anomalous fields shown in Fig. 5a and b are based on the first 50 years of the experiment (weak-AMOC) versus the control run. The grey bars indicate minimum differences between two 50-year ($n = 50$) averages taken from a timeseries

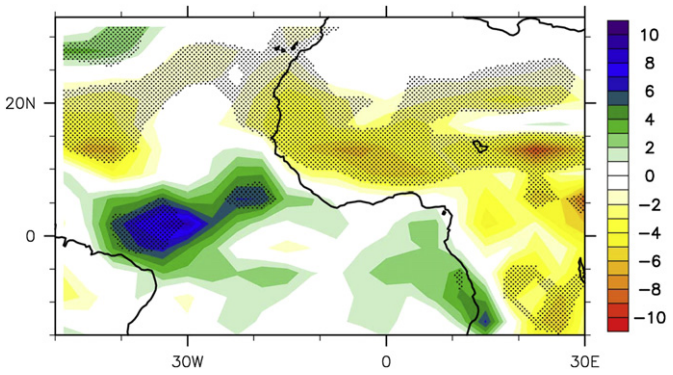

Fig. 7. Annual-mean precipitation anomaly (cm/a) of the intermediate-strength AMOC state. Shown is the average over model years 150–200 (grey box in Fig. 6) minus the long-term mean from the control run (strong-AMOC state). Stippling indicates statistical significance at the 0.05 level based on a *t*-test.

to the Atlantic Ocean, thus reducing continental rainfall in the western Sahel. This model outcome agrees with a number of studies demonstrating that the AEJ plays a key role in controlling sub-Saharan precipitation by transporting moisture off the continent below the level of condensation, thus increasing moisture divergence over North Africa (e.g. Rowell et al., 1992; Cook, 1999; Rowell, 2003; Cook and Vizy, 2006; Patricola and Cook, 2007; Mulitza et al., 2008; Patricola and Cook, 2008). In addition, Grist and Nicholson (2001) highlight the importance of the AEJ in governing dynamic instability mechanisms and hence convective activity over the West African Sahel. Provided that the state of strong AEJ is maintained long enough (e.g. due to a persistent North Atlantic meltwater input of moderate magnitude), it would contribute to the extended dry conditions over the western Sahel and explain the pollen distribution in core GeoB9508-5. The records presented in this study show that HS1 was one of the most severe and extensive dry periods lasting for over 4000 years. We discuss a succession of three phases during HS1 derived from both palynological data and model simulation. Phase 1 (~19–17.4 kyr BP) represents the onset of NE trade wind strengthening and dryness over the western Sahel, while phase 2 (~17.4–16.2 kyr BP) represents the millennial mid-HS1 interlude marked by relaxation of NE trade winds though aridity in the region is still severe. Phase 3 (~16.2–15 kyr BP) covers the last and extremely dry part of HS1 when NE trade winds were strongest. The total duration of the HS1 episode detected in the Sahel agrees (within age model uncertainties) with the temporal boundaries of Heinrich event *sensu lato* established by Stanford et al. (2011) which spans the entire period of the NADW collapse and includes three $\delta^{18}O$ phases that affected bottom waters.

Particularly, the extreme dryness during the later part of HS1 agrees with increased aridity observed further north in western Iberia during the latest phase of HS1 as revealed by a clear minimum in Mediterranean forest pollen (Sánchez Goñi et al., 2008) and the expansion of semi-desert plants (Naughton et al., 2009) indicating lower precipitation toward the end of HS1; as well as with increased dust fluxes off Mauritania suggesting extreme arid conditions and intensification of NE trade winds (Jullien et al., 2007). In contrast, on the western side of the Atlantic, the final phase of HS1 has (within age model uncertainties) a pronounced wet counterpart in NE Brazil where humid forest vegetation expanded in an otherwise semi-desert region between ~16.5 and 15 kyr BP that is suggestive of regional increases in precipitation (Dupont et al., 2010) (Fig. 4a). The development of wet

that are statistically significant (calculation based on the annual data using a *t*-test with $\alpha = 0.05$ significance level and assuming invariant standard deviation).

conditions in NE Brazil and also in the tropical Andes and parts of Amazonia (Peterson et al., 2000; Denton et al., 2010) suggests that the proposed sharp rainfall reduction over the western Sahel did not occur in South America. Since the modeled mid-tropospheric circulation anomaly extends over the entire tropical North Atlantic (Fig. 5b), the observed humid conditions probably reflect the consequence of an intensified AEJ, which affected the western Sahel climate by enhancing moisture export from the African realm. We hypothesize that it represents a large-scale rather than a regional change in the tropical atmospheric circulation, thus providing a link between West Africa and central/South America and may further explain the relationships between climate changes recorded on both sides of the Atlantic. However, to confirm this hypothesis there is a clear need for more high-resolution land–ocean correlation studies on both sides of the Atlantic in order to understand the impact of mid-level moisture transport over the tropical Atlantic which, so far, has gained little attention in paleo-hydroclimatological studies of the tropics.

6. Conclusions

The records presented in this study allow us to recognize three major phases within HS1 and to suggest potential forcing mechanisms for each. The general trend of extremely dry conditions associated with an intensification of the NE trade winds during HS1 is interrupted by an interval (between ~17.4 and 16.2 kyr BP) of reduced input of Saharan pollen and increased input of Sahelian pollen, which is interpreted as a period of NE trade wind relaxation associated with an intensification and a southward expansion of the AEJ. Occurring between two distinct NE trade wind maxima during the first and the latter part, this mid-HS1 interlude implies the dominance of the mid-tropospheric AEJ over low-level NE trade winds while dry conditions remained severe. The proposed scenario is supported by the results of a numerical modeling experiment indicating that the dynamics of the AEJ may largely be independent from the NE trade wind system. It shows that an intensified AEJ plays a key role in diverging moisture from the African realm to the Atlantic Ocean, thus reducing continental rainfall and extending aridity throughout the western Sahel during HS1.

Our results offer an important complement to recently published paleorecords from the region. They show that HS1 was one of the longest and most severe arid periods of the western Sahel and that the persistence of this millennial-scale Sahel drought must have involved an intensified and southward expanded AEJ in addition to a southward shift of the ITCZ. Whatever its exact cause, such a mechanism would have a considerable effect on low-latitude African climate and may provide a link between climate changes in West Africa and South America. A better understanding of the AEJ dynamics is pivotal to predict its fate and that of the Sahel during upcoming climate changes.

Acknowledgments

This work was funded through the Deutsche Forschungsgemeinschaft as part of the DFG-Research Center/Excellence cluster “The Ocean in the Earth System”. We thank the captain, the crew and participants of *R/V Meteor* cruise M65/1 for recovering the studied material. The manuscript benefited from constructive discussions and many valuable suggestions by J.F. McManus, H. Johnstone, K. Bogus, M. Koelling and J. Groeneveld. Thanks to M. Hoins for assistance with palynological processing. The climate model experiments were performed on the IBM pSeries 690 supercomputer of the Hochleistungsrechner Nord (HLRN). Data have been submitted to the Publishing Network for Geoscientific & Environmental Data (PANGAEA, www.pangaea.de).

Appendix A. Supplementary material

Supplementary material associated with this article can be found, in the online version, at http://dx.doi.org/10.1016/j.quascirev.2012.10.015.

References

Afiesimama, E.A., 2007. Annual cycle of the mid-tropospheric easterly jet over West Africa. Theor. Appl. Climatol. 90, 103–111.
Bard, E., Hamelin, B., Fairbanks, R.G., Zindler, A., 1990. Calibration of the ^{14}C time-scale over the past 30,000 years using mass spectrometric U–Th ages from Barbados corals. Nature 345, 405–410.
Bard, E., Rostek, F., Turon, J.L., Gendreau, S., 2000. Hydrological impact of Heinrich events in the subtropical Northeast Atlantic. Science 289, 1321–1324.
Bouimetarhan, I., Dupont, L., Schefuß, E., Mollenhauer, G., Mulitza, S., Zonneveld, K., 2009. Palynological evidence for climatic and oceanic variability off NW Africa during the late Holocene. Quat. Res. 72, 188–197.
Bonnefille, R., Riollet, G., 1980. Pollens des Savanes d'Afrique Orientale. Edition de CNRS, Paris, 140 pp., 113pl.
Broecker, W.S., McGee, D., Adams, K.D., Cheng, H., Laurence Edwards, R., Oviatt, C.G., Quade, J., 2009. A great Basin-wide dry episode during the first half of the Mystery interval? Quat. Sci. Rev. 28, 2557–2563.
Clark, P.U., Alley, R.B., Keigwin, L.D., Licciardi, J.M., Johnsen, S.J., Wang, H., 1996. Origin of the first global meltwater pulse following the last glacial maximum. Paleoceanography 11, 563–578.
Colarco, P.R., Toon, O.B., Reid, J.S., Livingston, J.M., Russel, P.B., Redmann, J., Schmid, B., Maring, H.B., Savoie, D., Welton, E.J., Campbell, J.R., Holben, B.N., Levy, R., 2003. Saharan dust transport to the Caribbean during PRIDE: 2. Transport, vertical profiles and deposition in simulations of in situ and remote sensing observations. J. Geophys. Res. 103, 8590.
Cook, K.H., 1999. Generation of the African Easterly Jet and its role in determining West African precipitation. J. Clim. 12, 1165–1184.
Cook, K.H., Vizy, E.K., 2006. Coupled model simulations of the West African monsoon system: 20th century simulations and 21st century predictions. J. Clim. 19, 3681–3703.
Dahl, K.A., Broccoli, A.J., Stouffer, R.J., 2005. Assessing the role of North Atlantic freshwater forcing in millenial scale climate variability: a tropical Atlantic Perspective. Clim. Dyn. 24, 325–346.
Denton, G.H., Anderson, R.F., Toggweiler, J.R., Edwards, R.L., Schaefer, J.M., Putnam, A.E., 2010. The Last Glacial termination. Science 328, 1652–1656.
Duplessy, J.C., Shackleton, N.J., 1985. Response of global deep-water circulation to earth's climatic change 135,000–107,000 years ago. Nature 316, 500–507.
Duplessy, J.C., Shackleton, N.J., Fairbanks, R.G., Labeyrie, L., Oppo, D., Kallel, N., 1988. Deepwater source variations during the last climatic cycle and their impact on the global deepwater circulation. Paleoceanography 3, 343–360.
Dupont, L.M., 1993. Vegetation zones in NW Africa during the brunhes chron reconstructed from marine palynological data. Quat. Sci. Rev. 12, 189–202.
Dupont, L.M., 1999. Pollen and spores in marine sediments from the east Atlantic. A view from the ocean into the African continent. In: Fischer, G., Wefer, G. (Eds.), Proxies in Paleoceanography, Examples from the South Atlantic. Springer, Berlin, pp. 523–546.
Dupont, L.M., Agwu, C.O.C., 1991. Environmental control of pollen grain distribution patterns in the Gulf of Guinea and offshore NW-Africa. Geolog. Rundsc. 80, 567–589.
Dupont, L.M., Hooghiemstra, H., 1989. The Saharan–Sahelian boundary during the Brunhes chron. Acta Bot. Neerland. 38, 405–415.
Dupont, L.M., Schütz, F., Teboh, E.C., Jennerjahn, T.C., Behling, H., Paul, A., 2010. Two-step vegetation response to enhanced precipitation in northeastern Brazil during Heinrich event 1. Glob. Change Biol. 16, 1647–1660.
Eynaud, F., Zaragosi, S., Scourse, J., Mojtahid, M., Bourillet, J.-F., Hall, I.R., Penaud, A., Locascio, M., Reijonen, A., 2007. Deglacial laminated facies on the NW European continental margin: the hydrographic significance of British–Irish Ice Sheet deglaciation and Fleuve Manche paleoriver discharges. Geochem. Geophys. Geosyst. 8. http://dx.doi.org/10.1029/2006GC001496
Faegri, K., Iversen, J., 1989. In: Faegri, K., Kaland, P.E., Krzywinski, K. (Eds.), Textbook of Pollen Analysis, fourth ed. Wiley, New York.
Fairbanks, R.G., 1989. A 17,000-year glacio-eustatic sea level record: influence of glacial melting rates on the Younger Dryas event and deep-ocean circulation. Nature 342, 637–642.
Fisher, R.A., 1925. Applications of “Student's” distribution. Metron 5, 90–104.
Gasse, F., 2000. Hydrological changes in the African tropics since the Last Glacial Maximum. Quat. Sci. Rev. 19, 189–211.
Gherardi, J., Labeyrie, L., McManus, J., Francois, R., Skinner, L., Cortijo, E., 2005. Evidence from NE Atlantic basin for variability in the rate of meridional overturning circulation through the last deglaciation. Earth Planet. Sci. Lett. 240
Gherardi, J., Labeyrie, L., Nave, S., Francois, R., McManus, J., Cortijo, E., 2009. Glacial–interglacial circulation changes inferred from 231Pa/230Th sedimentary record in the North Atlantic region. Paleoceanography 24, PA2204.
Grist, J.P., Nicholson, S.E., 2001. A study of the dynamic factors influencing rainfall variability in the West African Sahel. J. Clim. 14, 1337–1359.

Grousset, F.E., Cortijo, E., Huon, S., Herve, L., Richter, T., Burdloff, D., Duprat, J., Weber, O., 2001. Zooming in on Heinrich layers. Paleoceanography 16, 240–259.
Haug, G.H., Ganopolski, A., Sigman, D.M., Rosell-Mele, A., Swann, G.E.A., Tiedemann, R., Jaccard, S.L., Bollmann, J., Maslin, M.A., Leng, M.J., Eglinton, G., 2005. North Pacific seasonality and the glaciation of North America 2.7 million years ago. Nature 433, 821–825.
Hooghiemstra, H., 1988. Changes of major wind belts and vegetation zones in NW Africa 20,000–5000 yr B.P., as deduced from a marine pollen record near Cap Blanc. Rev. Palaeobot. Palynol. 55, 101–140.
Hooghiemstra, H., Agwu, C.O.C., 1986. Distribution of palynomorphs in marine sediments: a record for seasonal wind patterns over NW Africa and adjacent Atlantic. Geolog. Rundsc. 75, 81–95.
Hooghiemstra, H., Bechler, A., Beug, H.J., 1987. Isopollen maps for 18,000 yr BP of the Atlantic offshore of Northwest Africa: evidence for palaeo-wind circulation. Paleoceanography 2, 561–582.
Hooghiemstra, H., Lézine, A.M., Leroy, S.A.G., Dupont, L.M., Marret, F., 2006. Late Quaternary palynology in marine sediments: a synthesis of the understanding of pollen distribution patterns in the NW African setting. Quat. Int. 148, 29–44.
Hsu, C.P.F., Wallace, J.M., 1976. The global distribution in annual and semiannual cycles in precipitation. Month. Weather Rev. 104, 1093–1101.
Itambi, A.C., von Dobeneck, T., Mulitza, S., Bickert, T., Heslop, D., 2009. Millennial-scale North West African droughts relates to H Events and D O Cycles: evidence in marine sediments from off-shore Senegal. Paleoceanography 24, 001570. http://dx.doi.org/10.1029/2007/PA001570.
Jullien, E., Grousset, F., Hemming, S.R., Peck, V.L., Hall, I.R., Jeantet, C., Billy, I., 2006. Contrasting conditions preceeding MIS3 and MIS2 Heinrich events. Glob. Planet. Change 54, 225–238.
Jullien, E., Grousset, F., Malaizé, B., Duprat, J., Sanchez-Goni, M.-F., Eynaud, F., Charlier, K., Schneider, R., Bory, A., Bout, V., Flores, J.A., 2007. Low latitude "dusty events" vs. high-latitude "icy Heinrich events". Quat. Res. 68, 379–386.
Lambeck, K., Chappell, J., 2001. Sea level change during the last glacial cycle. Science 292, 679–686.
Lézine, A.M., 1989. Late Quaternary vegetation and climate of the Sahel. Quat. Res. 2, 317–334.
Lézine, A.M., 1996. La mangrove ouest africaine, signal des variations du niveau marin et des conditions régionales du climat au cours de la dernière déglaciation. Bull. Soc. Géol. 167, 743–752.
Lézine, A.M., Casanova, J., 1989. Pollen and hydrological evidence for the interpretation of past climates in tropical West Africa during the Holocene. Quat. Sci. Rev. 8, 45–55.
Lézine, A.M., Hooghiemstra, H., 1990. Land-sea comparisons during the last glacial–interglacial transition: pollen records from west tropical Africa. Palaeogeogr. Palaeoclimatol. Palaeoecol. 79, 313–331.
Lézine, A.M., Turon, J.L., Buchet, G., 1995. Pollen analyses off Senegal: evolution of the coastal palaeoenvironment during the last deglaciation. J. Quat. Sci. 10, 95–105.
Lippold, J., Mulitza, S., Mollenhauer, G., Weyer, S., Christl, M., 2012. Boundary scavenging at the east Atlantic margin does not negate use of Pa/Th to trace Atlantic overturning. Earth Planet. Sci. Lett. 333–334, 317–331.
McManus, J.F., François, R., Gherardi, J.-M., Keigwin, L.D., Brown-Leger, S., 2004. Collapse and rapid resumption of Atlantic meridional circulation linked to deglacial climate changes. Nature 428, 834–837.
Michel, P., 1973. Les basins des fleuves Sénégal et Gambie, in Etude Géomorphologique, rep. Institut de recherche pour le développent, Paris.
Mulitza, S., Bouimetarhan, I., Brüning, M., Freesemann, A., Gussone, N., Filipsson, H., Heil, G., Hessler, S., Jaeschke, A., Johnstone, H., Klann, M., Klein, F., Küster, K., März, C., McGregor, H., Minning, M., Müller, H., Ochsenhirt, W.T., Paul, A., Scewe, F., Schulz, M., Steinlöchner, J., Stuut, J.B., Tjallingii, R., Dobeneck, T., Wiesmaier, S., Zabel, M., Zonneveld, K., 2006. Report and Preliminary Results of Meteor Cruise M65/1, Dakar – Dakar, 11.06.–01.07.2005. Berichte, Fachbereich Geowissenschaften, Universität Bremen, No. 252, 149 pp.
Mulitza, S., Prange, M., Stuut, J.B., Zabel, M., von Dobeneck, T., Itambi, C.A., Nizou, J., Schulz, M., Wefer, G., 2008. Sahel megadroughts triggered by glacial slowdowns of Atlantic meridional overturning. Paleoceanography 23, PA 4206. http://dx.doi.org/10.1029/2008PA001637.
Naughton, F., Sánchez Goñi, M.F., Desprat, S., Turon, J.L., Duprat, J., Malaizé, B., Joli, C., Cortijo, E., Drago, T., Freitas, M.C., 2007. Present-day and past (last 25 000 years) marine pollen signal off western Iberia. Mar. Micropaleontol. 62, 91–114.
Naughton, F., Sánchez Goñi, M.F., Kageyama, M., Bard, E., Duprat, J., Cortijo, E., Desprat, S., Malaizé, B., Joly, C., Rostek, F., Turon, J.L., 2009. Wet to dry climatic trend in north-western Iberia within Heinrich events. Earth Planet. Sci. Lett. 284, 329–342.
Nicholson, S.E., 2009. On the factors modulating the intensity of the tropical rainbelt over West Africa. Int. J. Climatol. 29, 673–689.
Nicholson, S.E., Grist, J.P., 2003. The seasonal evolution of the atmospheric circulation over West Africa and Equatorial Africa. J. Clim. 16, 1013–1030.
Niedermeyer, E.M., Prange, M., Mulitza, M., Mollenhauer, G., Schefuß, E., Schulz, M., 2009. Extratropical forcing of Sahel aridity during Heinrich stadials. Geophys. Res. Lett. 36, L20707. http://dx.doi.org/10.1029/2009GL039687.
North Greenland Ice Core Project Members (NGRIP), 2004. High-resolution record of Northern Hemisphere climate extending into the last interglacial period. Nature 431, 147–151.
Patricola, C.M., Cook, K.H., 2007. Dynamics of the West African monsoon under mid-Holocene precessional forcing: regional climate model simulations. J. Clim. 20, 694–716.
Patricola, C.M., Cook, K.H., 2008. Atmosphere/vegetation feedbacks: a mechanism for abrupt climate change over northern Africa. J. Geophys. Res. 113, D18102. http://dx.doi.org/10.1029/2007JD009608.
Peck, V.L., Hall, I.R., Zahn, R., Elderfield, H., Grousset, F., Hemming, S.R., Scourse, J.D., 2006. High resolution evidence for linkages between NW European ice sheet instability and Atlantic Meridional Overturning Circulation. Earth Planet. Sci. Lett. 243, 476–488.
Penaud, A., Eynaud, E., Turon, J.-L., Blamart, D., Rossignol, L., Marret, F., Lopez-Martinez, C., Grimalt, J.O., Malaizé, B., Charlier, K., 2010. Contrasting paleoceanographic conditions off Morocco during Heinrich events (1 and 2) and the Last Glacial Maximum. Quat. Sci. Rev. 29, 1923–1939.
Peterson, L.C., Haug, G.H., Hughen, K.A., Röhl, U., 2000. Rapid changes in the hydrological cycle of the tropical Atlantic during the last Glacial. Science 290, 1947–1951.
Prange, M., 2008. The low-resolution CCSM2 revisited: new adjustments and a present day control run. Ocean Sci. 4, 151–181.
Prospero, J.M., 1990. Mineral–aerosol transport to the North Atlantic and North Pacific: the impact of African and Asian sources. In: Knap, A.H. (Ed.), The Long-range Atmospheric Transport of Natural and Contaminant Substances. Mathematical and Physical Sciences. Kluwer Academic Publishers, Dodrecht, pp. 59–86.
Prospero, J.M., Carlson, T.N., 1981. Saharan air outbreaks over the tropical North Atlantic. Pure Appl. Geophys. 119, 677–691.
Prospero, J.M., Nees, R.T., 1986. Impact of the North African drought and El Nino on mineral dust in the Barbados trade winds. Nature 320, 735–738.
Prospero, J.M., Ginoux, P., Torres, O., Nicholson, S.E., Gill, T.E., 2002. Environmental characterization of global sources of atmospheric soil dust identified with the nimbus 7 total zone mapping spectrometer (TOMS) absorbing aerosol product. Rev. Geophys. 40, 2-1–2–31.
Romero, O.E., Kim, J.-H., Donner, B., 2008. Submillenial-to-millenial variability of Diatom production off Mauritania, NW Africa, during the last glacial cycle. Paleoceanography 23, PA 3218. http://dx.doi.org/10.1029/2008PA001601.
Rowell, D.P., 2003. The impact of Mediterranean SSTs on the Sahelian rainfall Season. J. Clim. 16, 849–862.
Rowell, D.P., Folland, C.K., Maskell, K., Owen, J.A., Ward, M.N., 1992. Modelling the influence of global sea surface temperatures on the variability and predictability of seasonal Sahel rainfall. Geophys. Res. Lett. 19, 905–908.
Sánchez Goñi, M.F., Landais, A., Fletcher, W., Naughton, F., Desprat, S., Duprat, J., 2008. Contrasting impacts of Dansgaard–Oeschger oscillations over a western European latitudinal transect: implications for the location of main sources of glacial CH4. Quat. Sci. Rev. 27, 1136–1151.
Sarnthein, M., Koopmann, B., 1980. Late Quaternary deep-sea record on northwest African dust supply and wind circulation. Palaeoecol. Afr. 12, 239–253.
Sarnthein, M., Tetzlaff, G., Koopmann, B., Wolter, K., Pflaumann, U., 1981. Glacial and interglacial wind regimes over the eastern subtropical Atlantic and North-West Africa. Nature 293, 193–196.
Sarnthein, M., Thiede, J., Pflaumann, U., Erlenkeuser, H., Fütterer, D., Koopmann, B., Lange, H.E.S., 1982. Atmospheric and oceanic circulation patterns off Northwest Africa during the past 25 million years. In: Von Rad, U., Hinz, K., Sarnthein, M., Seibold, E. (Eds.), Geology of the Northwest African Continental Margin. Springer, Berlin, pp. 584–604.
Shackleton, N.J., Fairbanks, R.G., Chiu, T.-C., Parrenin, F., 2004. Absolute calibration of the Greenland time scale: implications for Antarctic time scales and for Δ14C. Quat. Sci. Rev. 23, 1513–1522.
Stanford, J.D., Rohling, E.J., Bacon, S., Roberts, A.P., Grousset, F.E., Bolshaw, M., 2011. A new concept for the paleoceanographic evolution of Heinrich event 1 in the North Atlantic. Quat. Sci. Rev. 30, 1047–1066.
Stouffer, R.J., Yin, J., Gregory, J.M., Dixon, K.W., Spelman, M.J., Hurlin, W., Weaver, A.J., Eby, M., Flato, G.M., Hasumi, H., Hu, A., Jungclause, J., Kamenkovich, I.V., Levermann, A., Montoya, M., Murakami, S., Nawrath, S., Oka, A., Peltier, W.R., Robitaille, D.Y., Sokolov, A., Vettoretti, G., Weber, S.L., 2006. Investigating the cause of the response of the thermohaline circulation to Past and future climate change. J. Clim. 19, 1365–1387.
Street-Perrott, F.A., Perrott, R.A., 1990. Abrupt climate fluctuations in the tropics: the influence of Atlantic Ocean Circulation. Nature 343, 607–611.
Stuut, J.-B., Zabel, M., Ratmeyer, V., Helmke, P., Schefuß,, E., 2005. Provenance of present-day eolian dust collected off NW Africa. J. Geophys. Res. 110, 4202–5161.
Tjallingii, R., Claussen, M., Stuut, J.B., Fohlmeister, J., Jahn, A., Bickert, T., Lamy, F., Röhl, U., 2008. Coherent high- and low-latitude control of the northwest African hydrological balance. Nat. Geosci. 1, 670–675.
Vincens, A., Lezine, A.M., Buchet, G., Lewden, D., le Thomas, A., 2007. African pollen data base inventory of tree and shrub pollen types. Rev. Palaeobot. Palynol. 145, 135–141.
White, F., 1983. The Vegetation of Africa. UNESCO, Paris, 384 pp.
World Resources Institute, 2003. http://www.wri.org/.
Zaragosi, S., Eynaud, F., Pujol, C., Auffret, G.A., Turon, J.L., Garlan, T., 2001. Initiation of European deglaciation as recorded in the northwestern Bay of Biscay slope environments (Meriadzek Terrace and Trevelyan Escarpment): a multi-proxy approach. Earth Planet. Sci. Lett. 188, 493–507.
Zarriess, M., Johnstone, H., Prange, M., Steph, S., Groeneveld, J., Mulitza, S., Mackensen, A., 2011. Bipolar seesaw in the northeastern tropical Atlantic during Heinrich stadials. Geophys. Res. Lett. 38, L04706. http://dx.doi.org/10.1029/2010GL046070.